



Download

Export

The Egyptian Journal of Radiology and Nuclear Medicine

Volume 48, Issue 1, March 2017, Pages 107-113

open access

Original Article

Reliability of multidetector CT in the diagnosis of cerebrospinal fluid rhinorrhea with operative correlation

Haisam Atta ^a  , Gehan S. Seifeldein ^b  , Momen AlMamoun ^c  , Hisham Imam ^b   **Show more**<https://doi.org/10.1016/j.ejrn.2016.12.005>[Get rights and content](#)Under a Creative Commons [license](#)

Abstract

Purpose

To evaluate the role of non-contrast multidetector CT in the diagnosis of CSF leaks and skull base defects in correlation to operative findings.

Materials and methods

Twenty patients clinically diagnosed to have CSF rhinorrhea; 8 spontaneous and 12 post-traumatic patients were evaluated using 64-rows MDCT with slice section 0.6 mm. CT is considered accurate if correctly determine the site and size of bony defect as matched with operative findings.

Results

MDCT accurately detected the site of presumed CSF leak in 19 out of 20 cases with sensitivity 95%. Cribiform plate defect is the most common site of defect in 40% of cases with 75% of cases categorized as Keros type II. The consensus image with fair agreement ($K = 0.38$) shows that coronal reformat has the highest diagnostic performance in 75% of cases while the least diagnostic value is encountered with the axial plane in 15% of cases ($p = 0.095$). There is almost a perfect agreement ($K = 0.810$) between the MDCT measurements and operative size of bony defect with minimal difference in 10% of patients ($P < 0.001$).

Conclusion

Looking for relevant research?

Visit your personalized recommendations page

[View Recommendations](#)

Non-contrast MDCT is an accurate reliable non-invasive imaging modality for preoperative evaluation of CSF rhinorrhea.

[< Previous](#)[Next >](#)

Keywords

MDCT-CSF rhinorrhoea

1. Introduction

The passage of [cerebrospinal fluid](#) (CSF) through an osseous defect within the skull base is termed as CSF [rhinorrhea](#) [1].

The clinical importance of a CSF leak is recognized where the patients may be presented with a wide variety of symptoms including clear nasal discharge and headache or develop complications like [meningitis](#), [pneumocephalus](#) or even brain [abscess](#) [2], [3], [4].

Many classifications have been employed for CSF rhinorrhea based upon the [etiology](#) or clinical presentation. However, the most widely accepted classification system was described by Ommaya in 1960 dividing CSF leaks into traumatic or non-traumatic categories [5]. While the spontaneous type of CSF rhinorrhea is a separable entity that is considered when there is no discernible etiology could be detected, Even that some authors are referring to its etiology to be caused by [intracranial hypertension](#) or attribute it to multiple skull base defects [6].

Management of patients with CSF rhinorrhea remains controversial. Most studies recommend either an [endoscopic](#) or a transcranial surgical repair of CSF leaks [4], [7].

In Either approaches, Prompt identification of CSF [fistulae](#) and successful [surgical treatment](#) are critical for avoiding life-threatening complications [8].

A variety of imaging modalities including isotope scans, cross-sectional [computed tomography](#) (CT), and magnetic resonance (MR) [imaging techniques](#) have been employed to localize and characterize skull base defects that are presumed to be responsible for CSF leakage. However, still, there is no gold standard imaging modality, reflecting the difficulty of such diagnosis [1], [2], [3], [4], [5], [7], [8], [9], [10].

Multidetector CT (MDCT) involves rapid, continuous and isotropic volumetric acquisition improving the spatial and temporal resolution for three-dimensional and multiplanar reformations providing [image guidance](#) for operative repair [1], [11], [12].

Our aim is to evaluate the role of non-contrast MDCT reliability in localizing CSF leaks and skull base defects in correlation to operative findings.

2. Patients and methods

2.1. Study population characteristics

This prospective study was conducted during the period between 2014 and 2016 using a 64-row multidetector scanner, Ethics committee approval in addition to informed written consent from all patients were obtained.

Twenty consecutive patients presumed to have CSF [rhinorrhea](#). All these patients have positive $\beta 2$ [transferrin](#) activity from their nasal secretion confirming the presence of CSF nature.

Headache was the presenting symptom in the majority; [pneumocephalus](#) was present in 10 patients, [meningitis](#) in 3 patients and [hydrocephalus](#) in 1 patient.

Patients were divided according to their clinical presentation where rhinorrhea was considered active when continuous dripping is encountered or inactive if the dripping was intermittent.

All patients underwent imaging after the failure of one-week conservative treatment in the form of complete bed rest, oral acetazolamide, [diuretic](#) and prophylactic [antibiotics](#), the patients subjected to this study were eight males (40%) and 12 female patients (60%) their age ranged from 26 to 57 years with mean 39.3 ± 8.3 years. The most common age group encountered as ranging from 41 to 45 years (5 patients). No patients were excluded from our study.

2.2. CT technique

All scans were obtained on a 64-rows multidetector scanner (light VCT, GE Medical Systems), No IV [contrast material](#) was administered. Patients were within the machine with head first position in a supine position. Unenhanced scans were obtained from the level of skull vault to the mandible. The scanning parameters were done with automated tube current modulation (mA); 140 kVp; pitch 1.3.

The reconstruction parameters were adjusted as follows helical thickness 0.625 mm; pitch 0.98; speed 39.3; rotation time 0.8; FOV adjusted to large; standard and bone plus reconstruction was used; gantry angle zero.

Studies were transferred to GE Advantage workstation (ADW 4.4).

2.3. Image interpretation

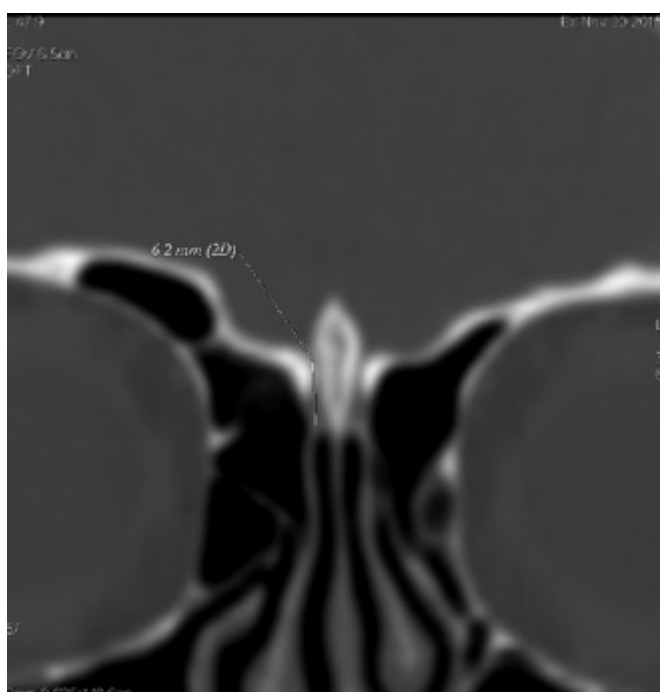
All studies were stripped of patient names; consensus interpretation by three radiologists [with experience 5–12 years after M.D.] Reviewed the reconstructed images and actively manipulated each case for evaluating the site of bony defect and comparing the diagnostic performance of each plane.

The three radiologist were blinded to each other reports and the operative findings which were performed after imaging by median duration nine days.

The MDCT findings suggestive of a CSF leak include a defect in the skull base bone with partial opacification of the nearby [sinus](#) [1].

The axial, sagittal and coronal reformats are revised, with increased slice thickness to 4.2 mm in a bone algorithm. The diagnostic performance of each plane is noted as diagnostic if it clearly demonstrates the bone defect, or confirmatory if it confirms the site but it by itself does not clarify the lesion alone or even no role if does not add value to the characterization of the location of the bony defect.

If a bony defect is present, the anatomical location of the defect and its size are recorded. Also, the variation of the [olfactory](#) fossa depth is determined by the depth of the [cribriform plate](#) and graded according to Keros classification, whereas 1–3 mm was graded as type I, depth of 4–7 mm is graded as type II while a depth of 8–16 mm is graded as type III [13], [14] (Fig. 1).



[Download high-res image \(85KB\)](#) [Download full-size image](#)

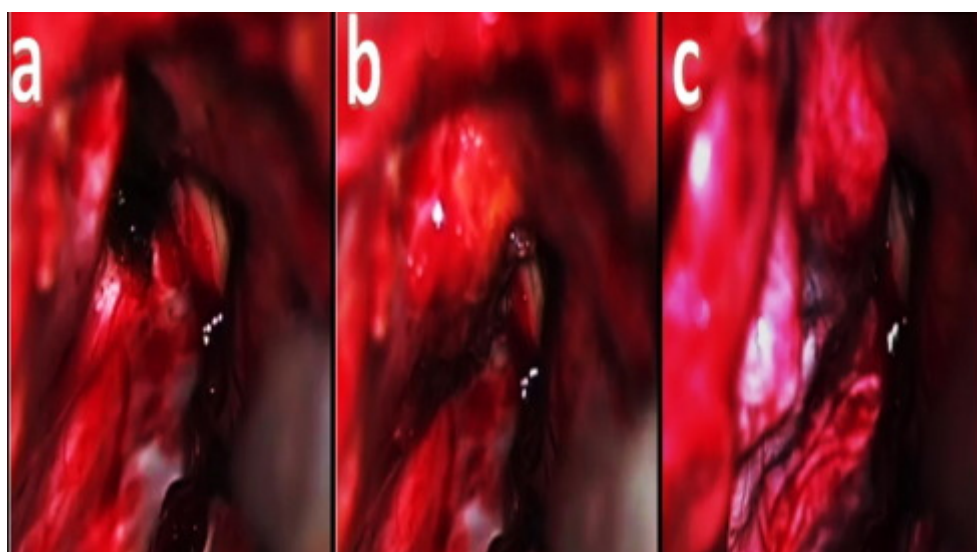
Fig. 1. Measurement of the depth of [olfactory](#) fossa to be graded according to Keros, in this case, depth = 6.2 mm and accordingly graded as Keros type II.

2.4. Surgical technique

All patients performed [surgical management](#) of the fistulous tract with nine days median duration (range from 2 to 23 days) after imaging.

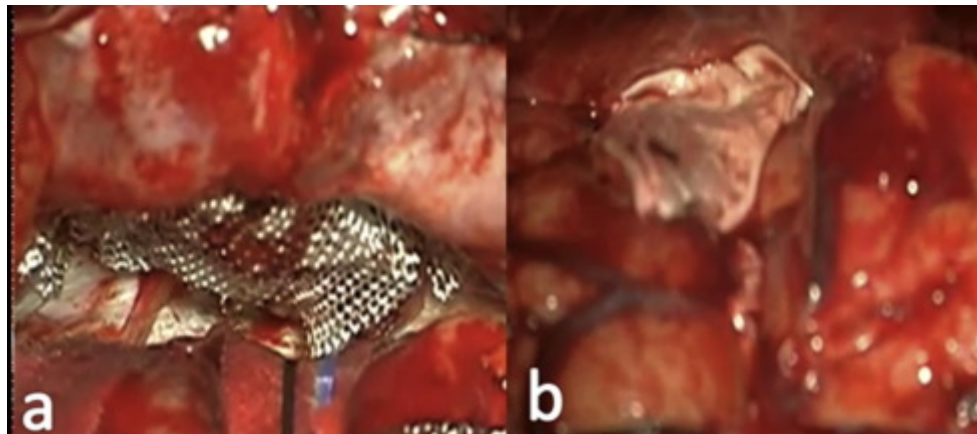
In the majority of our patients (18 (90%) patients), the frontal transcranial intradural approach was used where a pericranium flap was first prepared, the patients were placed in the supine position, a unilateral [craniotomy](#) via a coronal incision on the affected side. For a proper exploration of the cranial base, the craniotomy was made as low as possible. The [frontal lobe](#) was elevated, and [dura](#) was opened exploring the anterior cranial fossa to

locate the [fistula](#). The defect was identified; its size was recorded using a surgical tap graded in millimeters. The pericranium was folded to cover it and sutured to the cranial base dura. The bone flap was repositioned, fixed and closure was performed ([Fig. 2](#), [Fig. 3](#)).



[Download high-res image \(110KB\)](#) [Download full-size image](#)

Fig. 2. Operative images of (a) Identification of the site of the defect at the [cribriform plate](#). (b) Blugging a pad of fat into the defect (c) inserting pericranial flap.



[Download high-res image \(115KB\)](#) [Download full-size image](#)

Fig. 3. Operative images of a case (a) Placement of pad of fat at the site of skull base defect. (b) Placement of pericranial flap.

In two patients, following [transsphenoidal surgery](#) CSF rhinorrhea was treated by redo microscopic transsphenoidal approach where sealing of the defect with [fascia](#) lata and tissue glue in addition to nasal packing for at least two days.

The surgical findings were used as a standard reference, the confirmation of diagnosis, the size of the defect and correlation with the accuracy of location. Comparison of diagnostic

yield of each reformatted plane is recorded.

2.5. Statistical analysis

The imaging and operative data were collected and verified by the researchers after coding in an Excel sheet program. Conversion to the SPSS program version 16 for statistical analysis; employing descriptive statistics, chi-square test. Fleiss Kappa was performed for correlation of the consensus interpretation of the three radiologists regarding the three different planes while Cohen kappa is used to determine the correlation of the imaging and operative size. A significant p-value was considered statistically significant if less than 0.05.

3. Results

3.1. Clinical classification

The twenty patients were classified into 13 active cases with continuous dripping and seven inactive cases with intermittent dripping. According to the patients' history, spontaneous nasal dripping found in 8 (40%) cases while traumatic **etiology** is encountered in 12 (60%) cases out of which **iatrogenic** etiology found in 2(10%) cases following transsphenoidal **pituitary** operation.

The cross tabulation between site and type of leakage was summarized in [Table 1](#) that had no significant statistical values ($p = 0.777$).

Table 1. relation of type of leakage with site of bony defect.

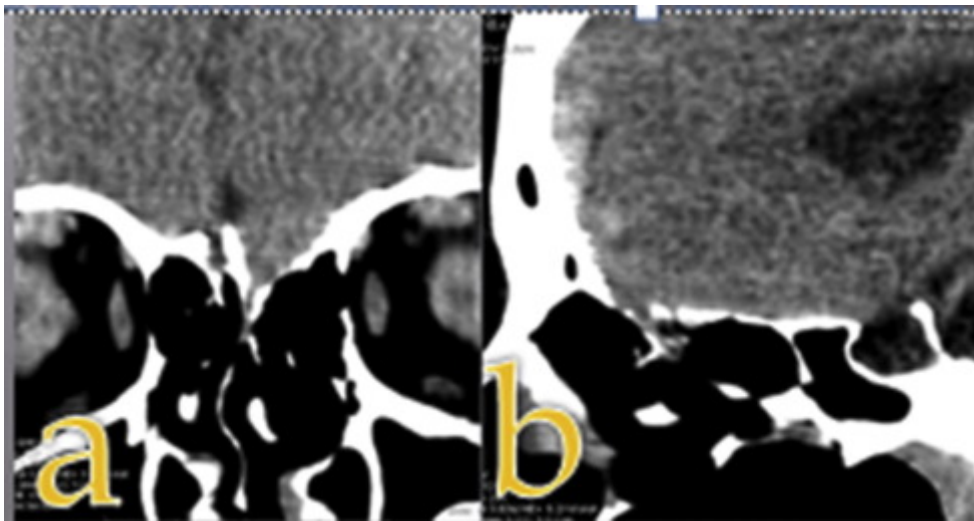
Site	Activity		Total
	Active	Inactive	
Cribriform plate	6	2	8
Fovea ethmoidal	1	1	2
Frontal sinus	2	1	3
Junction cribriform plate and fovea	1	2	3
Spheroidal sinus	3	1	4
Total	13	7	20

3.2. MDCT findings

The preoperative MDCT correctly detected 19 out of 20 cases rendering the sensitivity 95%. The missed case had recurrent **rhinorrhea** postoperatively secondary to dural defects.

3.2.1. Site of bony defects

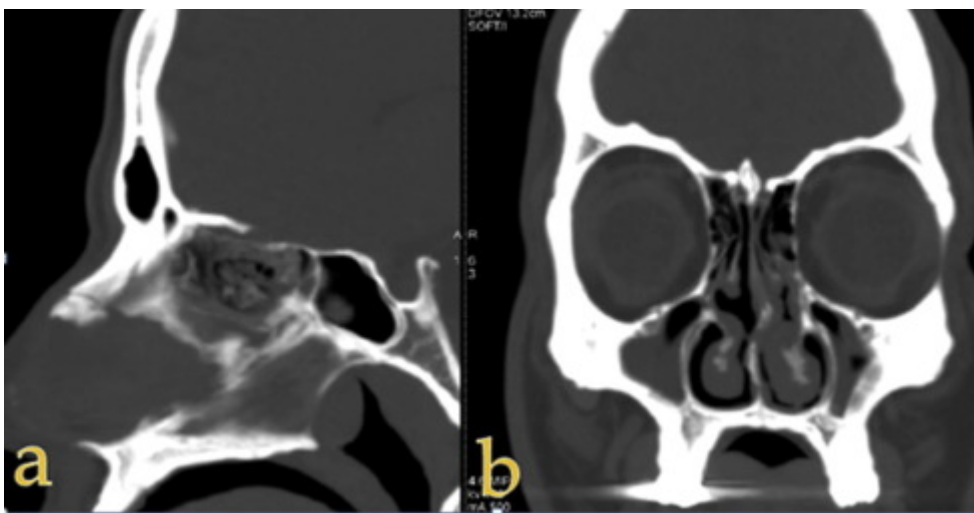
MDCT detected bony defects as follows: 8 (40%) cases in **cribriform plate** (Fig. 4, Fig. 5), 2 cases (10%) in **fovea ethmoidal**, 3 cases (15%) in **frontal sinus**, 3 cases (15%) in the junction of the cribriform plate and fovea ethmoidal and 4 (20%) cases in the **sphenoidal sinus**. The only missed case was located in sphenoidal sinus where it is presented with an intermittent leak.



[Download high-res image \(121KB\)](#)

[Download full-size image](#)

Fig. 4. Bony defect at the right **cribriform plate** with diagnostic performance of coronal plane (a) with clarification Keros type II and the confirmatory role of the sagittal plane(b).



[Download high-res image \(93KB\)](#)

[Download full-size image](#)

Fig. 5. Diagnostic performance of coronal plane of the bony defect at the right **cribriform plate** and clarification of depth of **olfactory groove** as type I (b) with and the confirmatory role of the sagittal plane.

Majority of patients of study group 75% was categorized as Keros type II while 25% was categorized as Keros type I.

3.2.2. Diagnostic performance of different radiological planes according to the consensus interpretation

Each radiologist evaluated each single regarding its diagnostic role and consensus interpretation revealed a fair agreement with $K = 0.38$ according to Fleiss Kappa.

The consensus interpretation showed that there were variable roles of each orthogonal plane (Table 2). However, Coronal reformat had the highest diagnostic performance in 75% of cases (Table 3) while the sagittal plane has a dominant confirmatory role in 65% of cases (Table 4). On the other hand, the least diagnostic value is encountered with the axial plane in 15% of cases (Table 5) (see Fig. 6, Fig. 7).

Table 2. Diagnostic performance of different planes according to consensus interpretation.

Plane	Diagnostic role					
	Coronal		Axial		Sagittal	
	N.	%	N.	%	N.	%
Confirmatory	5	25	4	20	13	65
Diagnostic	15	75	3	15	5	25
No value	1	5	15	75	5	25

^aThe consensus interpretation may show more than one role for the single orthogonal plane.

Table 3. Crosstabulation of the diagnostic consensus of diagnostic performance of different plane with the site of the bony defect.

Diagnostic performance of each plane ^a	Site of defect					Total
	Cribriform plate	Fovea ethmoidal	Frontal sinus	Junction cribriform plate and fovea	Sphenoidal sinus	
Axial	0	0	2	0	1	3
Coronal	8	2	1	3	1	15
Sagittal	2	0	1	0	2	5

P value = 0.095 (not significant).

^a

The consensus interpretation showed more than one role for the single orthogonal plane.

Table 4. Crosstabulation of the diagnostic consensus of the confirmatory performance of different plane with the site of the bony defect.

Confirmatory performance of each plane ^a	Site of defect					Total
	Cribriform plate	Fovea ethmoidal	Frontal sinus	Junction cribriform plate and fovea	Sphenoidal sinus	
Axial	2	0	1	0	1	4
Coronal	1	0	0	3	1	5
Sagittal	6	3	1	1	2	13

P value = 0.428 (not significant).

a

The consensus interpretation showed more than one role for the single orthogonal plane.

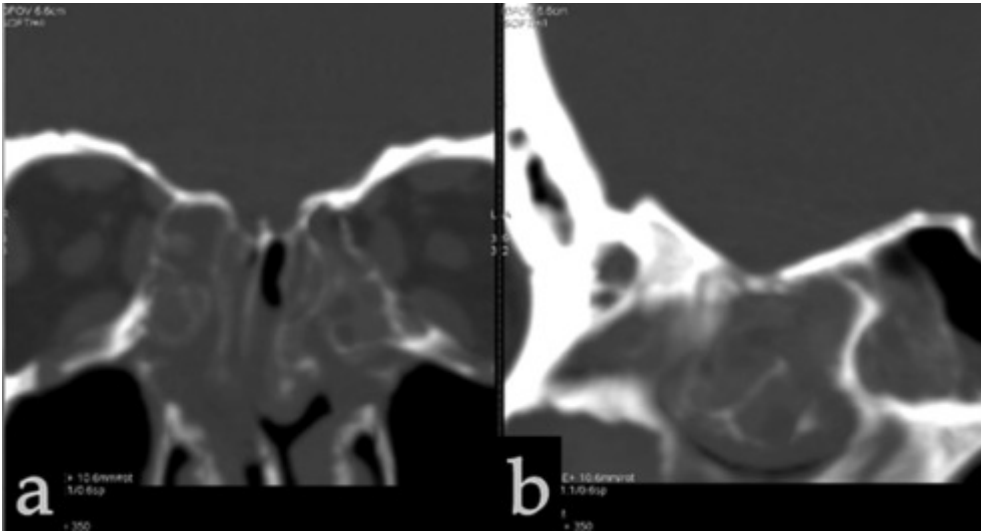
Table 5. Crosstabulation of the diagnostic consensus of no diagnostic role of the different plane with the site of the bony defect.

Absent diagnostic value of each plane ^a	Site of defect					Total
	Cribriform plate	Fovea ethmoidal	Frontal sinus	Junction cribriform plate and fovea	Sphenoidal sinus	
Axial	6	4	1	2	2	15
Coronal	0	0	0	1	0	1
Sagittal	1	1	1	1	1	5

P value = 0.08 (not significant).

a

The consensus interpretation showed more than one role for the single orthogonal plane.



[Download high-res image \(73KB\)](#)[Download full-size image](#)

Fig. 6. Sinonasal polypi with a superimposed fungal infection where the diagnostic role is in the sagittal plane (b) and the confirmatory role of the coronal plane (a) with a demonstration of Keros type II.

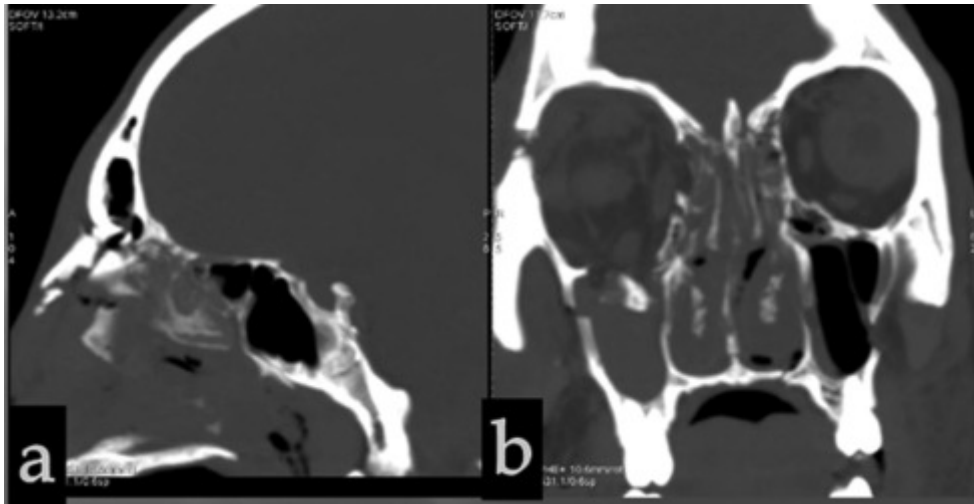
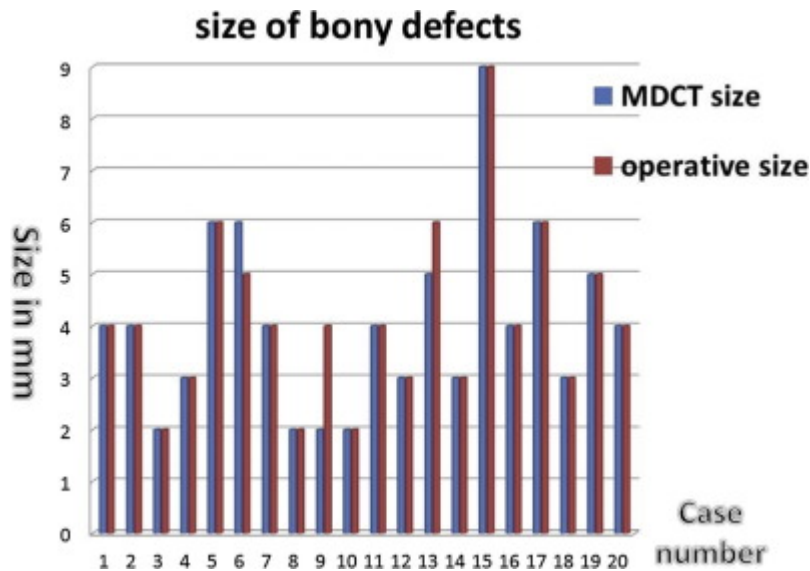
[Download high-res image \(89KB\)](#)[Download full-size image](#)

Fig. 7. Post-traumatic status with a bony defect at the junction of the left cribriform plate and Fovea ethmoidal with diagnostic performance of coronal plane (a) with type II Keros grading and the confirmatory role of the sagittal plane (b).

No significant statistical values were encountered with the diagnostic role of each plane ($p = 0.095$) or the confirmatory role of each orthogonal plane ($p = 0.428$) or even the absence of diagnostic role of different planes ($p = 0.08$) according to the consensus interpretation of the three radiologists.

3.2.3. The size of bony defect

There is almost perfect agreement ($K = 0.810$) between the MDCT measurements and operative size of bony defect with minimal difference in 10% of patients ($P < 0.001$). As the operative size was exceeding the imaging size by 2 mm in one case while the other case, the MDCT size exceeded that of operative estimate by 1 mm (Fig. 8).



[Download high-res image \(150KB\)](#)

[Download full-size image](#)

Fig. 8. Graphic presentations of the imaging and operative size of bony defects among the study population.

4. Discussion

CSF [rhinorrhea](#) represents an important clinical entity in which 50% of affected patients will be at risk of developing [meningitis](#) [15].

Imaging can precisely detect the exact location of leakage site which is considered the key to successful treatment [16]. Although there is no imaging “gold standard” for diagnosis of such important entity reflecting the difficulty with this diagnosis [1].

The use of MDCT can provide the surgeon with accurate information regarding the site and size of the skull base defect [17]. Even that Shetty et al. [14] stated that CT is the mainstay in imaging due to its ability to resolve osseous structures and recorded sensitivity of 92% while our results recorded a higher sensitivity to detect lesions with 95%.

The aim of imaging is to confirm the diagnosis, with possible evaluation of the underlying cause in addition to localization and characterization of the bony defect size prior to surgery [1]. Active manipulation of the imported images regarding the window level and width allow accurate localization of skull bony defects and estimation of the size of the defect, to enable proper [surgical preparation](#) to block the defect [1], [11]. MDCT is the routine imaging tool for detection of bony defects in CSF rhinorrhea, [MRI](#) may be indicated to exclude [encephalocele](#) [4]. In the current study, the size of defects was quite small with no suspicious of occurrence of encephalocele. Although heavily weighted T2WI may be indicated to clarify the site of active leakage, in unclear cases with active CSF leakage [1]. While post [contrast MRI](#) is reserved for cases of suspected complicated meningitis or presence of cerebral space occupying lesions [4]. Both entities were not present in our

study population as no clinical manifestations of the former or imaging findings of the latter cause, and thus we did not use postcontrast studies.

One of our cases presented with [hydrocephalus](#). However, none of our cases is presented with empty sella Syndrome nor signs of benign increased [intracranial tension](#) as slit [ventricles](#) or tonsillar ectopia [13]. This finding is not consistent with Shetty et al. [14] where in their Study the prevalence of empty sella was 63%.

In our study population; 60% of our patients were females, their majority 7 cases (87.5%) encountered as spontaneous leakage. This fact is in agreement with Schlosser et al. [13]. On the other hand Yilmazlar et al. [18] reported traumatic [etiology](#) represents 90% of their cases; however, it represents only 60% of our study population, among which there are 3 cases with multiple lesions.

These study results are in agreement with Ulmer et al. [19] when stating that CT is the preferred technique for detecting and delineating bony landmarks and anatomical variants. However, most of our cases are recorded to be Keros type II variant; while ElAbri et al. [20] stated that Keros type III is the most common type expected to develop CSF rhinorrhea.

Our results show that the most common site of the bony defect is the [cribriform plate](#) (40%) whereas Scholsem et al. [8] found a high percentage of leaks through an [ethmoid](#), cribriform plate fracture (87%). Although Tolly et al. [21] stated that detection of the bony defects are harder due to thinning of the cribriform plate and lamella, however, the contralateral comparison is helpful. Also, asymmetrical thinning with an overlying soft tissue or mucosal thickening beneath are useful in the detection of the lesion at this site [3].

In spite that using the consensus interpretation in the current study with a fair agreement and regarding the fact that with consensus diagnosis; it is difficult to compare between studies [22].

[Frontal sinus](#) posterior walls, as well as the mastoid complex and posterolateral walls of the [sphenoid sinus](#), are best evaluated by axial images [2], [3], [4], [5], [8], [9], [10]. On the contrary, our results show that axial images had the least diagnostic value by 15% and recorded no diagnostic value in 75%.

While evaluation of the cribriform plates, [ethmoidal](#) roof, and sphenoid sinuses necessitates the employment of coronal images [2], [3], [4], [5], [8], [9], [10]. This is in agreement with our results where coronal have the highest diagnostic accuracy in 75% of patients and plays a confirmatory role in 25%.

On the other hand, Sagittal plane in the current study results show a predominant confirmatory role in 65% of cases and have a diagnostic role in 25% of cases, where the highest diagnostic role is encountered when the defect is located in the sphenoid sinus. This is in agreement with Ulmer et al. [19] when stating that CT allows a proper evaluation of the sphenoid sinus.

The results of current study show almost perfect agreement between MDCT and operative measurements. This is quite similar to La Fatta et al. [16] when stating that CT osseous defects measurements are accurate, although they were employing endoscopic measurements while we used operative measurements.

The transcranial approach utilized in the majority of our patients, employing a pericardial graft and fixation is achieved with suturing and tissue glue in an attempt to avoid failure of grafting and to release. While sphenoid sinus is packing with a fascia lata graft and tissue glue with the microscopic transsphenoidal approach. These results are in agreement with Liu et al. [7], Krishnan et al. [23] and Nishioka et al. [24].

Where Liu et al. [7] reported that autologous tissue is better than artificial dural tissue to repair fistulae as it offers the best compatibility and facilitates optimal wound healing.

While Krishnan et al. [23] stated that tensor fascia lata a musculofascial flap is an excellent source of a vascularized muscle flap. On the other hand, Nishioka et al. [24] for the repairing of CSF leaks recommended direct suturing augmented by the use of fibrin glue for sellar packing.

Among the limitation of our study is the small number of cases as the trend for the treatment of such cases in our locality is conservative rather than operative management. Non employment of a low KV dose technique is an another limitation.

5. Conclusion

Non-contrast MDCT is an accurate, reliable non-invasive imaging modality for preoperative evaluation of CSF rhinorrhea.

Conflict of interest

None of the Authors are having any conflict of interest to declare.

[Recommended articles](#)

[Citing articles \(0\)](#)



References

- [1] K.M. Lloyd, J.M. DelGaudio, P.A. Hudgins
Imaging of skull base cerebrospinal fluid leaks in adults 1
Radiology, 248 (2008), pp. 725-736
[CrossRef](#) [View Record in Scopus](#)
- [2] B. Aarabi, L.G. Leibrock
Neurosurgical approaches to cerebrospinal fluid rhinorrhea
Ear Nose Throat J, 71 (1992), pp. 300-305
[View Record in Scopus](#)
- [3] T. Asano, K. Ohno, Y. Takada, R. Suzuki, K. Hirakawa, S. Monma

Fractures of the floor of the anterior cranial fossa


J Trauma Acute Care Surg, 39 (1995), pp. 702-706

[CrossRef](#)

- [4] E. Mohamed, A.A. Ibrahim, E.A. Ihab, S. Elwany, M.H. Hassab, H.M. Khamis
Evaluation of the role of high resolution computed tomography and magnetic resonance cisternography in preoperative identification of skull base defect in cases of cerebrospinal fluid rhinorrhea
Int Med J Malay, 11 (2012)
- [5] M.K. Wax, H.H. Ramadan, O. Ortiz, S.J. Wetmore
Contemporary management of cerebrospinal fluid rhinorrhea
Otolaryngol Neck Surg, 116 (1997), pp. 442-449
[Article](#)  [Download PDF](#) [CrossRef](#) [View Record in Scopus](#)
- [6] S.M. Lieberman, S. Chen, D. Jethanamest, R.R. Casiano
Spontaneous CSF rhinorrhea: prevalence of multiple simultaneous skull base defects
Am J Rhinol Allergy, 29 (2015), p. 77
[CrossRef](#) [View Record in Scopus](#)
- [7] P. Liu, S. Wu, Z. Li, B. Wang
Surgical strategy for cerebrospinal fluid rhinorrhea repair
Oper Neurosurg, 66 (2010), pp. ons281-ons286
[CrossRef](#)
- [8] M. Scholsem, F. Scholtes, F. Collignon, P. Robe, A. Dubuisson, B. Kaschten, *et al.*
Surgical management of anterior cranial base fractures with cerebrospinal fluid fistulae: a single-institution experience
Neurosurgery, 62 (2008), pp. 463-471
[CrossRef](#)
- [9] M.N.H. Lloyd, P.M. Kimber, E.H. Burrows
Post-traumatic cerebrospinal fluid rhinorrhoea: modern high-definition computed tomography is all that is required for the effective demonstration of the site of leakage
Clin Radiol, 49 (1994), pp. 100-103
[Article](#)  [Download PDF](#) [View Record in Scopus](#)
- [10] V. Lund, L. Savy, G. Lloyd, D. Howard
Optimum imaging and diagnosis of cerebrospinal fluid rhinorrhoea
J Laryngol Otol, 114 (2000), pp. 988-992
[View Record in Scopus](#)
- [11] S.J. McMahon, P.A. Hudgins
Management of cerebrospinal fluid leaks
Curr Opin Otolaryngol Head Neck Surg, 8 (2000), pp. 32-36
[CrossRef](#) [View Record in Scopus](#)
- [12] C. Meco, G. Oberascher
Comprehensive algorithm for skull base dural lesion and cerebrospinal fluid fistula diagnosis

Laryngoscope, 114 (2004), pp. 991-999

[CrossRef](#) [View Record in Scopus](#)

- [13] R.J. Schlosser, W.E. Bolger
Nasal cerebrospinal fluid leaks
J Otolaryngol, 31 (2002), pp. S28-S37
[View Record in Scopus](#)
- [14] P.G. Shetty, M.M. Shroff, G.M. Fatterpekar, D.V. Sahani, M.V. Kirtane
A retrospective analysis of spontaneous sphenoid sinus fistula: MR and CT findings
Am J Neuroradiol, 21 (2000), pp. 337-342
[View Record in Scopus](#)
- [15] J.A. Stone, M. Castillo, B. Neelon, S.K. Mukherji
Evaluation of CSF leaks: high-resolution CT compared with contrast-enhanced CT and radionuclide cisternography
Am J Neuroradiol, 20 (1999), pp. 706-712
[View Record in Scopus](#)
- [16] V. La Fata, N. McLean, S.K. Wise, J.M. DelGaudio, P.A. Hudgins
CSF leaks: correlation of high-resolution CT and multiplanar reformations with intraoperative endoscopic findings
Am J Neuroradiol, 29 (2008), pp. 536-541
[CrossRef](#) [View Record in Scopus](#)
- [17] M. Prokop
General principles of MDCT
Eur J Radiol, 45 (2003), pp. S4-S10
[Article](#)  [Download PDF](#)
- [18] S. Yilmazlar, E. Arslan, H. Kocaeli, S. Dogan, K. Aksoy, E. Korfali, *et al.*
Cerebrospinal fluid leakage complicating skull base fractures: analysis of 81 cases
Neurosurg Rev, 29 (2006), pp. 64-71
[CrossRef](#) [View Record in Scopus](#)
- [19] S. Ulmer, E. Schulz, B. Moeller, U.R. Krause, A. Nabavi, H.M. Mehdorn, *et al.*
Radiation dose of the lens in trans-sphenoidal pituitary surgery: pros and cons of a conventional setup using fluoroscopic guidance and CT-based neuronavigation
Am J Neuroradiol, 28 (2007), pp. 1559-1564
[CrossRef](#) [View Record in Scopus](#)
- [20] R. Al-Abri, D. Bhargava, W. Al-Bassam, Y. Al-Badaai, S. Sawhney
Clinically significant anatomical variants of the paranasal sinuses
Oman Med J, 29 (2014), pp. 110-113
[CrossRef](#) [View Record in Scopus](#)
- [21] M.R. Chaaban, E. Illing, K.O. Riley, B.A. Woodworth
Spontaneous cerebrospinal fluid leak repair: a five-year prospective evaluation
Laryngoscope, 124 (2014), pp. 70-75

[CrossRef](#) [View Record in Scopus](#)

- [22] A.A. Bankier, D. Levine, E.F. Halpern, H.Y. Kressel
Consensus interpretation in imaging research: is there a better way? 1
Radiology, 257 (2010), pp. 14-17
[CrossRef](#) [View Record in Scopus](#)
- [23] K.G. Krishnan, P.A. Winkler, A. Müller, G. Grevers, H.-J. Steiger
Closure of recurrent frontal skull base defects with vascularized flaps—a technical case report
Acta Neurochir (Wien), 142 (2000), pp. 1353-1358
[CrossRef](#) [View Record in Scopus](#)
- [24] H. Nishioka, H. Izawa, Y. Ikeda, H. Namatame, S. Fukami, J. Haraoka
Dural suturing for repair of cerebrospinal fluid leak in transnasal transsphenoidal surgery
Acta Neurochir (Wien), 151 (2009), pp. 1427-1430
[CrossRef](#) [View Record in Scopus](#)

Peer review under responsibility of The Egyptian Society of Radiology and Nuclear Medicine.

© 2016 The Egyptian Society of Radiology and Nuclear Medicine. Production and hosting by Elsevier.

ELSEVIER

[About ScienceDirect](#) [Remote access](#) [Shopping cart](#) [Contact and support](#)
[Terms and conditions](#) [Privacy policy](#)

We use cookies to help provide and enhance our service and tailor content and ads. By continuing you agree to the [use of cookies](#).

Copyright © 2018 Elsevier B.V. or its licensors or contributors. ScienceDirect® is a registered trademark of Elsevier B.V.

 **RELX** Group™